

r^2 SCAN-D4: Dispersion corrected meta-generalized gradient approximation for general chemical applications

Cite as: J. Chem. Phys. **154**, 061101 (2021); <https://doi.org/10.1063/5.0041008>

Submitted: 21 December 2020 . Accepted: 18 January 2021 . Published Online: 09 February 2021

 Sebastian Ehlert,  Uwe Huniar,  Jinliang Ning,  James W. Furness,  Jianwei Sun,  Aaron D. Kaplan,  John P. Perdew, and  Jan Gerit Brandenburg



View Online



Export Citation



CrossMark



New

Your Qubits. Measured.

Meet the next generation of quantum analyzers

- Readout for up to 64 qubits
- Operation at up to 8.5 GHz, mixer-calibration-free
- Signal optimization with minimal latency

[Find out more](#)



Zurich Instruments

r²SCAN-D4: Dispersion corrected meta-generalized gradient approximation for general chemical applications

Cite as: J. Chem. Phys. 154, 061101 (2021); doi: 10.1063/5.0041008

Submitted: 21 December 2020 • Accepted: 18 January 2021 •

Published Online: 9 February 2021











View Online



Export Citation



CrossMark

Sebastian Ehlert,¹  Uwe Huniar,²  Jinliang Ning,³  James W. Furness,³  Jianwei Sun,³ 
Aaron D. Kaplan,⁴  John P. Perdew,^{4,5}  and Jan Gerit Brandenburg^{6,a)} 

AFFILIATIONS

¹Mulliken Center for Theoretical Chemistry, University of Bonn, Beringstr. 4, 53115 Bonn, Germany

²Biovia, Dassault Systèmes Deutschland GmbH, Imbacher Weg 46, 51379 Leverkusen, Germany

³Department of Physics and Engineering Physics, Tulane University, New Orleans, Louisiana 70118, USA

⁴Department of Physics, Temple University, Philadelphia, Pennsylvania 19122, USA

⁵Department of Chemistry, Temple University, Philadelphia, Pennsylvania 19122, USA

⁶Enterprise Data Office, Merck KGaA, Frankfurter Str. 250, 64293 Darmstadt, Germany

^{a)} Author to whom correspondence should be addressed: j.g.brandenburg@gmx.de

ABSTRACT

We combine a regularized variant of the strongly constrained and appropriately normed semilocal density functional [J. Sun, A. Ruzsinszky, and J. P. Perdew, Phys. Rev. Lett. 115, 036402 (2015)] with the latest generation semi-classical London dispersion correction. The resulting density functional approximation r²SCAN-D4 has the speed of generalized gradient approximations while approaching the accuracy of hybrid functionals for general chemical applications. We demonstrate its numerical robustness in real-life settings and benchmark molecular geometries, general main group and organo-metallic thermochemistry, and non-covalent interactions in supramolecular complexes and molecular crystals. Main group and transition metal bond lengths have errors of just 0.8%, which is competitive with hybrid functionals for main group molecules and outperforms them for transition metal complexes. The weighted mean absolute deviation (WTMAD2) on the large GMTKN55 database of chemical properties is exceptionally small at 7.5 kcal/mol. This also holds for metal organic reactions with an MAD of 3.3 kcal/mol. The versatile applicability to organic and metal-organic systems transfers to condensed systems, where lattice energies of molecular crystals are within the chemical accuracy (errors <1 kcal/mol).

Published under license by AIP Publishing. <https://doi.org/10.1063/5.0041008>

I. INTRODUCTION

The quantum mechanical description of physical and chemical materials at the electronic resolution is an increasingly important task for *in silico* simulations. Here, density functional theory (DFT) has emerged in the past decades as one of the most versatile methodological frameworks.^{1,2} This leading position in both materials and chemical applications is largely due to the excellent accuracy over the computational cost ratio as well as the broad applicability across system classes of today's density functional approximations (DFAs).³⁻⁵

The Jacob's ladder hierarchy⁶ is commonly used to classify DFAs. In this hierarchy, DFAs are systematically improved by ascending rungs of different approximations: the local density approximation (LDA), generalized gradient approximations (GGAs), meta-GGAs, hybrid functionals (including a fraction of nonlocal exact exchange), and double-hybrid functionals (including nonlocal correlation). In terms of efficiency, meta-GGAs are in a favorable spot, as they have the same cubic scaling with the system size as LDA. Yet, many of the meta-GGAs proposed so far cannot truly leverage the full potential of their rung. Some shortcomings of the existing functionals are increased sensitivity to the

numeric integration grid as observed in the strongly constrained and appropriately normed (SCAN) functional⁷ or several Minnesota type functionals,^{8–10} purely empirical parameters as present in the B97M functional,¹¹ and sensitivity to the kinetic energy density.^{12,13} Recent developments of semi-local DFAs combine exact constraints with various degrees of parametrization to improve descriptions of short- to medium-range electron correlation.^{7,14,15}

The SCAN functional⁷ is constructed to rigorously satisfy all known exact constraints suitable for a meta-GGA. While the functional itself has shown excellent performance in previous studies, the severe numerical instabilities inherent to the functional impeded its adoption for many computational studies. With the recently proposed regularized SCAN (rSCAN)¹⁶ and the subsequent restoration of exact constraints in r²SCAN,¹⁷ the main drawback of the SCAN functional seems to be resolved. Shortcomings of the SCAN functional might still be present in its successors, rSCAN and r²SCAN. Notably, the description of water clusters (H₂O)_n (2 ≤ n ≤ 8) show the overbinding tendency of SCAN.¹⁸ A recent work by Sharkas *et al.*,¹⁸ however, demonstrates that this can be mended by the Perdew–Zunger self-interaction correction (PZ-SIC). SCAN and r²SCAN show similar behaviors for self-interaction error prone systems, which may make r²SCAN amenable to a PZ-SIC correction as well. However, r²SCAN is often more accurate than SCAN, as in the extensive benchmarking here, in the atomization energies of molecules¹⁷ and in the spin-crossover energies of molecules.¹⁹

Nevertheless, semilocal functionals cannot include long-range correlation effects such as London dispersion interactions.²⁰ To truly judge its applicability, we extensively tested r²SCAN combined with the state-of-the-art D4 dispersion correction,²¹ which shows unprecedented performance for a range of diverse chemical and physical properties. To investigate the development of the SCAN-type functionals, we include both SCAN-D4 and rSCAN-D4 in the comparison to r²SCAN-D4 and can attribute improvements in non-covalent interactions (NCIs) mainly to the regularization and improvements in thermochemistry and barrier heights to the restoration of the exact constraints.

We give a concise methodological overview (Sec. II) on r²SCAN and D4 before testing the full method against established DFAs over a wide range of benchmarks (Sec. III), with particular focus on molecular geometries, thermochemistry, kinetics, and non-covalent interactions in small and large complexes.

II. METHODS

The rSCAN¹⁶ functional regularizes the severe numerical instability or inefficiency of the otherwise successful SCAN⁷ functional at the expense of breaking exact constraints SCAN was constructed to obey. This problem arises in many codes that employ localized basis sets and is less problematic in many codes that employ plane wave basis sets. While numerical challenges are indeed resolved, a rigorous adherence to exact constraints is core to the design of the SCAN functional and likely important for transferable accuracy across domains of applicability.¹⁹ This seems to be reflected in rSCAN's relatively poor performance for molecular atomization energies compared to other tests.^{22,23} The r²SCAN functional¹⁷

combines the good accuracy of SCAN with the numerical efficiency of rSCAN by directly restoring exact constraint satisfaction to the rSCAN regularizations.

The SCAN functional is constructed as an interpolation between single orbital and slowly varying energy densities designed to maximize exact constraint satisfaction.⁷ The interpolation is controlled by an iso-orbital indicator

$$\alpha = \frac{\tau - \tau_W}{\tau_U}, \quad (1)$$

where $\tau_W = |\nabla\rho|^2/(8\rho)$ and $\tau_U = 3(3\pi^2)^{2/3}\rho^{5/3}/10$ are the von Weizsäcker and uniform electron gas kinetic energy densities, respectively.²⁴ In subsequent studies, α has been shown to contribute to numerical instability.^{25,26} To remove these effects, a regularized α' was used in rSCAN that removes single orbital divergences at the expense of breaking exact coordinate scaling conditions^{27–29} and the uniform density limit. These conditions are restored in r²SCAN by adopting a different regularization,

$$\tilde{\alpha} = \frac{\tau - \tau_W}{\tau_U + \eta\tau_W}, \quad (2)$$

where $\eta = 10^{-3}$ is a regularization parameter.

The second regularization made in the rSCAN functional is to substitute the twisted piece-wise exponential interpolation of the original SCAN with a smooth polynomial function. This removes problematic oscillations in the exchange-correlation potential but introduces spurious terms in the slowly varying density gradient expansion that deviate from the exact expansion^{30,31} recovered by SCAN. A corrected gradient expansion term is used in r²SCAN that cancels these spurious terms, so the functional recovers the slowly varying density gradient expansion to the second order. A recent modification of SCAN for improved bandgap accuracy from Aschbrock and Kümmel named “TASK”³² is able to enforce the fourth-order gradient expansion for the exchange energy without apparent numerical problems,³³ resolving the dominant source of numerical inefficiency. The importance of the fourth-order exchange terms is not established, however, and we are thus satisfied using one less exact constraint compared to SCAN. TASK uses an LSDA for correlation, however, and consequently violates many important exact constraints for correlation, e.g., the second order gradient expansion, that are obeyed by SCAN and r²SCAN.

A. Numerical stability

Numerical instabilities are revealed by SCAN's sensitivity to the choice of the numerical integration grid, often requiring dense computationally costly grids.^{16,25,34} This issue has been addressed with the rSCAN and r²SCAN functionals. Figure 1 shows that the regularization indeed leads to two orders of magnitude error reduction when comparing r²SCAN with SCAN. This holds for both total energy and nuclear gradients for all chosen numerical settings. In practice, this allows for more computationally favorable settings. To give a rough estimate of the computational cost of r²SCAN compared to SCAN, we consider system 10 of the S30L³⁵ with 158 atoms and 8250 atomic orbitals in a def2-QZVP basis set. A SCAN calculation using Turbomole's grid 4 and a rad size of 50 (8.5 × 10⁶

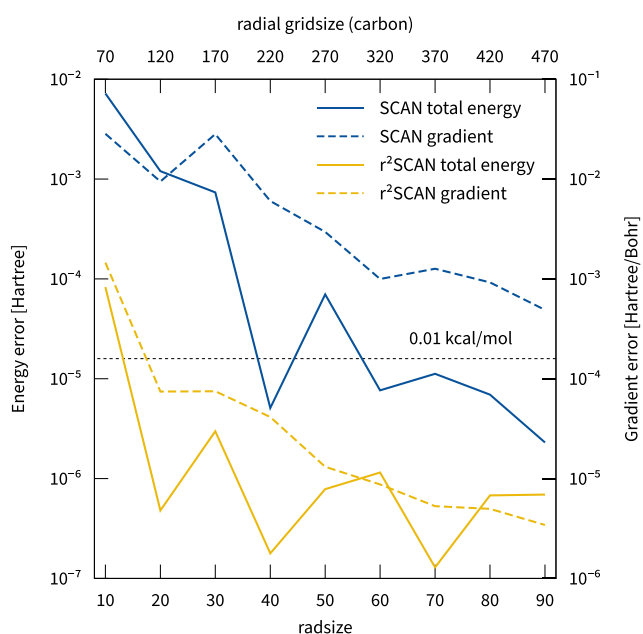


FIG. 1. Errors for FeCp_2 with SCAN/def2-QZVP and r^2 SCAN/def2-QZVP using different radial grid sizes. For both methods, grid four and SCF convergence criteria of 10^{-7} Hartree are used and the radial grid size was varied. The reference has a rad size of 100 or radial grid size of 515, 520, and 535 for hydrogen, carbon, and iron, respectively. The gradient error is the sum of the absolute errors of all gradient components. For further explanation, see the end of Sec. II A.

grid points) would take ~ 10 h, while an r^2 SCAN calculation with the Turbomole grid m4 and a rad size of 6 (1.6×10^6 grid points) takes only three and a half hours for the same numerical accuracy, resulting in a computational saving of a factor of three to five.³⁶ We recommend using r^2 SCAN with a rad size of 6 and potentially increasing it to 10 for problematic geometry optimizations.³⁷ We also compared SCAN and r^2 SCAN with different energy cutoffs in a PAW expansion and found that r^2 SCAN is not as sensitive as SCAN, i.e., the total energy converges significantly faster.³⁸

B. Training of damping functions

As London dispersion interactions arise from nonlocal electron correlations, they cannot be captured by any meta-GGA. In the past years, a range of schemes have been developed to capture these interactions in the DFT framework.^{20,39–43} Here, we combine r^2 SCAN with the semi-classical D4 dispersion correction.²¹ Its energy contribution is calculated by

$$E_{\text{disp}}^{\text{D4}} = -\frac{1}{2} \sum_{n=6,8}^{\text{atoms}} \sum_{A,B} s_n \frac{C_n^{\text{AB}}}{R_{\text{AB}}^n} \cdot f_n^{\text{BJ}}(R_{\text{AB}}) - \frac{1}{6} \sum_{A,B,C}^{\text{atoms}} s_9 \frac{C_9^{\text{ABC}}}{R_{\text{ABC}}^9} \cdot f_9^{\text{BJ}}(R_{\text{ABC}}, \theta_{\text{ABC}}), \quad (3)$$

TABLE I. D3(BJ) and D4 damping parameter for r SCAN and r^2 SCAN functionals.

Model		s8	a1	a2/Bohr	RMS ^a
rSCAN	D3(BJ)-ATM	1.0886	0.4702	5.7341	0.31
	D4(EEQ)-ATM	0.8773	0.4911	5.7586	0.30
r^2 SCAN	D3(BJ)-ATM	0.7898	0.4948	5.7308	0.28
	D4(EEQ)-ATM	0.6019	0.5156	5.7734	0.28

^aRoot-mean-square error in kcal/mol of dispersion corrected density functionals on the fit set S66X8,⁴⁵ S22X5,⁴⁹ and NCIBLIND.⁵⁰

where R_{AB} is the atomic distance, C_n^{AB} is the n -th order dispersion coefficient, and $f_n^{\text{BJ}}(R_{\text{AB}})$ is the Becke–Johnson damping function.^{44,45} R_{ABC} and C_9^{ABC} denote the geometrically averaged distance and dispersion coefficient, respectively, and θ_{ABC} is the angle dependent term of the triple-dipole contribution.^{46,47} The s_8 parameter for the two-body dispersion and the a_1 and a_2 parameters entering the critical radius in the damping function are adjusted to match the local description of a specific DFA. Damping parameters are fitted using a Levenberg–Marquardt least-squares minimization to reference interaction energies, as described in Ref. 21. Optimized parameters are given in Table I. The b parameters for r SCAN-VV10 and r^2 SCAN-VV10 were determined to be 10.8 and 12.3, respectively, on the same set.^{42,51}

C. Computational details

All ground state molecular DFT calculations were performed with a development version of Turbomole.^{52,53} The resolution of identity (RI) approximation^{54,55} was applied in all calculations for the electronic Coulomb energy contributions. For all functionals except SCAN, Turbomole’s modified grids of type m4 were used. For all SCAN calculations, grid 4 with an increased radial integration size of 50 was used instead. Self-consistent field convergence criteria of 10^{-7} Hartree were applied. Ahlrichs’ type quadruple-zeta basis sets, def2-QZVP,⁵⁶ were used throughout if not stated otherwise.

The periodic electronic structure calculations were conducted with $\text{VASP}_{6.1}$ ^{57,58} with projector-augmented plane waves (PAWs) with an energy cutoff of 800 or 1000 eV (hard PAWs^{59,60}). Tight self-consistent field settings and large integration (and fine FFT) grids are used. The Brillouin zone sampling has been increased to converge the interaction energy to 0.1 kcal/mol. The non-periodic directions use a vacuum spacing of 12 Å.

III. RESULTS

A. Bond length and molecular geometries

To evaluate the description of covalent bond distances, we compare experimental and calculated ground-state equilibrium distances R_e (in pm) for 35 light main group bonds (LMGB35⁶¹), 11 heavy main group bonds (HMGB11⁶¹), and 50 bonds in 32 3d transition metal complexes (TMC32⁶²). Additionally, we investigate

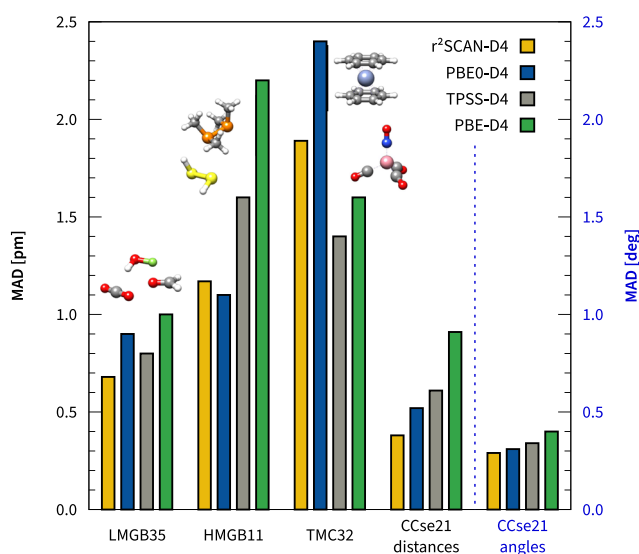


FIG. 2. Errors in the bond length from r^2 SCAN-D4 and other DFAs separated into light main group bonds (LMGB35⁶¹), heavy main group bonds (HMGB11⁶¹), transition metal complexes (TMC32⁶²), and semi-experimental organic molecules (CCse21⁶³). PBE0-D4, TPSS-D4, and PBE-D4 results for the first three sets are taken from Ref. 21.

the bond distances and angles for a set of simple organic molecules against accurate semi-experimental Refs. 63 and 64. Extended statistics and optimized geometries are made freely available.⁶⁵

We include r^2 SCAN-D4, PBE0-D4,⁶⁶ TPSS-D4,⁶⁷ and PBE-D4⁶⁸ in the comparison shown in Fig. 2. For organic molecules, we find exceptional performance for all functionals, with errors smaller than 1 pm in the bond distances and half a degree in the bond angles. While all methods reproduce the reference values closely, we observe the best agreement from r^2 SCAN-D4 with a mean absolute deviation (MAD) of 0.4 pm and 0.3° for the bond distances and angles, respectively. For light main group elements, all methods give a mean absolute deviation of less than 1 pm as well, which was also observed in previous studies.^{21,25} In comparison with the other methods tested here, r^2 SCAN-D4 also yields the lowest MAD of only 0.7 pm. Finally, for transition metal complexes, r^2 SCAN-D4 performs reasonably well with an MAD of 1.9 pm. Overall, the performance of r^2 SCAN is similar to, and sometimes even better than, the hybrid PBE0-D4, which in turn is one of the best performing hybrid functionals for molecular geometries.⁶¹

B. General main group thermochemistry and non-covalent interactions

To investigate the performance of r^2 SCAN-D4 for general main group chemistry, we use the main group thermochemistry, kinetics, and non-covalent interactions (GMTKN55) database.⁶⁹ The GMTKN55 database is a compilation of 55 benchmark sets to assess the performance of DFAs and allows a comprehensive comparison of DFAs. It contains five categories: namely, basic properties, barrier heights, isomerizations and reactions, and intermolecular and

intramolecular non-covalent interactions (NCIs), see Fig. 3 for a performance overview of selected methods. Usual weighted total MADs (WTMAD2s) range from 2 kcal/mol to 3 kcal/mol for double hybrid functionals, over 3 kcal/mol–4 kcal/mol for hybrid functionals to 8 kcal/mol–9 kcal/mol for (meta-)GGAs, while the lowest rung functionals such as PWLDA yield WTMADs of 17 kcal/mol on the GMTKN55. With the exception of the semi-empirical B97M-V¹¹ (and its B97M-D4 variant⁷⁰), r^2 SCAN-D4 is the best non-hybrid functional on the GMTKN55 so far with a WTMAD2 of 7.5 kcal/mol, compared to other meta-GGAs such as SCAN-D4 (8.61 kcal/mol) or TPSS-D4 (9.36 kcal/mol). For the isomerization and reaction category as well, as for the intramolecular NCIs, r^2 SCAN-D4 can even compete with the performance of the hybrid PBE0-D4 (WTMAD2 6.66 kcal/mol).

We additionally evaluated r^2 SCAN-D4 and SCAN-D4⁷¹ on the GMTKN55 set to monitor the development in the SCAN-family of functionals. The main difference between SCAN-D4 and r^2 SCAN-D4 is the general improvement in the description of non-covalent interactions, while both functionals perform similarly well in all other categories. Here, r^2 SCAN-D4 improves for both NCI categories with a weighted MAD of 6.8 kcal/mol over SCAN-D4, which yields a weighted MAD of 7.6 kcal/mol. This improvement in r^2 SCAN-D4 is mainly responsible for the smaller WTMAD2 of 8.3 kcal/mol compared to the WTMAD2 of 8.6 kcal/mol for SCAN-D4. For r^2 SCAN-D4, the improved description of NCI in r^2 SCAN-D4 is preserved (weighted MAD of 6.6 kcal/mol), but r^2 SCAN-D4 bests its predecessor in all three remaining categories, resulting in its exceptional WTMAD2 of 7.5 kcal/mol. The mindless benchmark (MB16-43 subset of GMTKN55) is specifically useful for testing a method's robustness to deal with the unusual chemistry in artificial molecules. Here, we see that enforcing exact constraints in non-empirical DFAs yields generally lower errors for artificial molecules than their empirical counterparts (see Table II).

To stress the importance of including a dispersion correction, we test the plain dispersion-uncorrected r^2 SCAN, which yields a significantly worse WTMAD2 of 8.8 kcal/mol, a difference similar in magnitude to the improvement from SCAN-D4 to r^2 SCAN-D4. In summary, r^2 SCAN-D4 shows a systematic improvement over its predecessor SCAN-D4 in all categories of GMTKN55 and can preserve improvements present in r^2 SCAN-D4. This makes r^2 SCAN-D4 one of the best non-empirical meta-GGAs that have been broadly benchmarked so far.

C. Beyond main group chemistry

Metal organic chemistry is one of the major application areas of non-hybrid DFAs. Here, we use the MOR41 benchmark set that contains 41 closed-shell metal-organic reactions representing common chemical reactions relevant in transition-metal chemistry and catalysis.⁷² We compare the statistical deviations from high-level references of r^2 SCAN-D4 to PBE0-D4, TPSS-D4, and PBE-D4 in Table III. The r^2 SCAN-D4 functional is one of the best meta-GGAs tested so far on the MOR41 benchmark set, with an MAD of 3.3 kcal/mol. While the SCAN-D4 method provides a slightly lower MAD, the analysis of other statistical quantities, such as the standard deviation (SD) and the maximum absolute error (AMAX), suggests less systematic results compared to r^2 SCAN-D4. This is confirmed by the Gini coefficient,⁷³ which is 0.44 for r^2 SCAN-D4 and 0.50

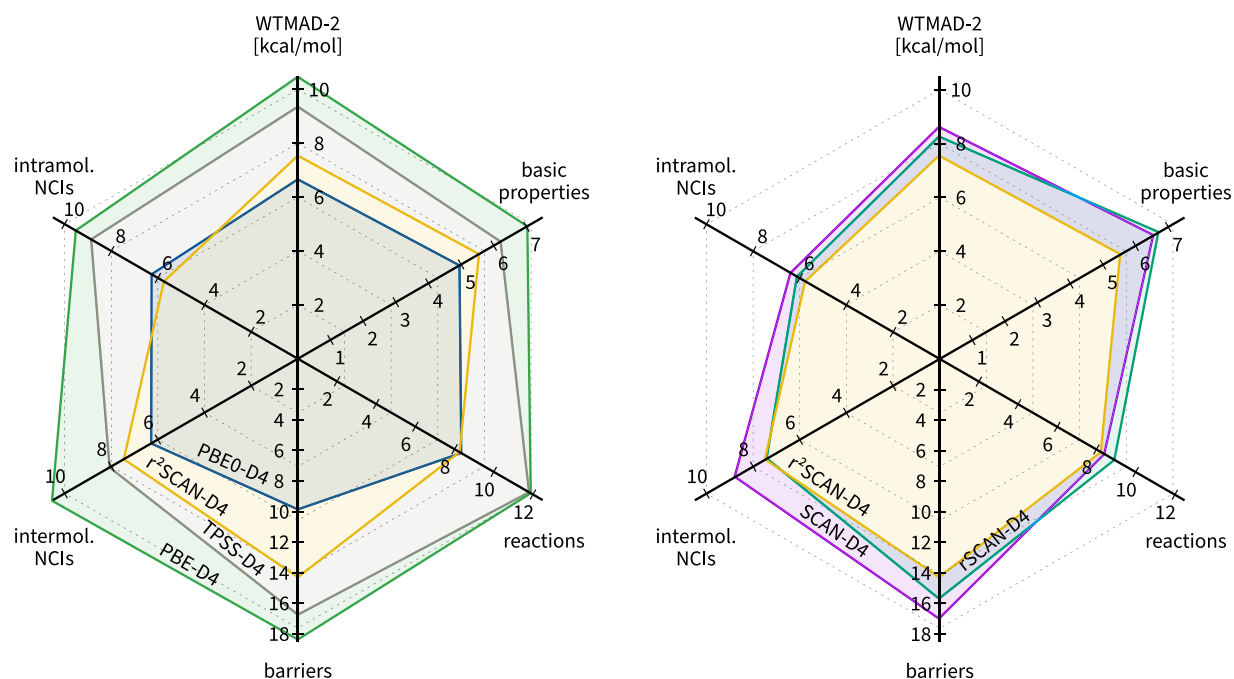


FIG. 3. Weighted mean absolute deviations of r^2 SCAN-D4 compared to other DFAs for the large database of general main group thermochemistry, kinetics, and non-covalent interactions GMTKN55.⁶⁹ On the left-hand side panel, r^2 SCAN-D4 is compared against functionals representative of their respective rungs. On the right-hand side panel, r^2 SCAN-D4 is compared to other members of the SCAN family, namely, r SCAN-D4 and SCAN-D4.

for SCAN-D4. Compare this to B97M-D4, one of the best meta-GGAs tested on the GMTKN55 set, which yields a larger MAD of 3.8 kcal/mol.⁷⁰

D. Non-covalent interactions in large complexes and molecular crystals

With the improved description of non-covalent interactions (NCIs), while retaining the computational efficiency of a meta-GGA, r^2 SCAN-D4 is a promising choice for interaction and association energies of large complexes. The results for the S30L,³⁵ L7,⁷⁴ and X40 $\times 10^{75}$ benchmark set are shown in Fig. 4.

TABLE II. Comparison of a few non-empirical and empirical dispersion corrected DFAs for the MB16-43 subset (artificial molecules) of GMTKN55. The non-empirical DFAs yield generally lower MADs (in kcal/mol) indicating better transferability across diverse systems.

Non-empirical DFA	MAD	Empirical DFA	MAD
r^2 SCAN-D4	14.6	MN15L	20.5
SCAN-D4	17.3	M06L	63.9
TPSS-D4	25.8	M06L-D4	62.6
PBE-D4	25.1	B97M-D4	37.5
PBE0-D4	16.0	B3LYP-D4	28.4

We choose the recently revised L7 benchmark⁷⁴ set to assess the performance of r^2 SCAN-D4 against local natural orbital based coupled cluster including singles, doubles, and perturbative triple excitations in the complete basis set limit [LNO-CCSD(T)/CBS].⁷⁶ Close agreement with an MAD of 0.9 kcal/mol is reached for r^2 SCAN-D4. This is a significant improvement over other meta-GGAs such as SCAN-D4 and TPSS-D4 with MADs of 1.3 kcal/mol and 1.4 kcal/mol, respectively.

We also investigated the description of association energies for large supramolecular complexes using the S30L benchmark set.³⁵ SCAN-D4 proved to be one of most accurate meta-GGAs in the previous benchmarks,²¹ giving a remarkable MAD of 2.0 kcal/mol,

TABLE III. Reaction energies of 41 metal-organic reactions compared to high-level.⁷² The MD, MAD, SD, and AMAX are given in kcal/mol, while the GINI coefficient is dimensionless.⁷³

	MD	MAD	SD	AMAX	GINI
r^2 SCAN	2.1	4.4	5.6	17.3	0.46
r^2 SCAN-D4	-0.2	3.3	4.3	14.0	0.44
SCAN-D4	-0.8	3.2	4.5	14.1	0.50
TPSS-D4	-1.5	3.5	4.4	22.6	0.39
PBE0-D4	-0.3	2.3	3.1	14.2	0.46
PBE-D4	-0.1	3.5	4.8	22.7	0.45

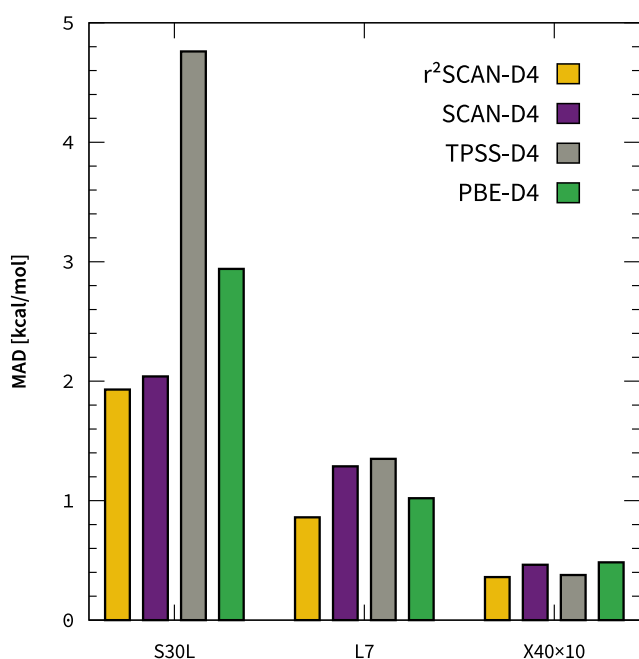


FIG. 4. Non-covalent interaction energies of host-guest systems, large systems, and halogen-bonded systems from r^2 SCAN-D4 compared to high-level references as well as other DFAs.

close to the uncertainty of the provided reference interactions; r^2 SCAN-D4 further improves upon this.

In particular, the association energies of the halogen-bonded complexes (15 and 16) are improved with r^2 SCAN-D4. The same trend can be observed in the HAL59 benchmark set of the GMTKN55, which shows an MAD of 1.0 kcal/mol with SCAN-D4 and improves with r^2 SCAN-D4 to an MAD of 0.8 kcal/mol. To confirm this trend, we additionally evaluated the X40 × 10 benchmark⁷⁵ containing 40 halogen bond dissociation curves with SCAN-D4 and r^2 SCAN-D4. Again, r^2 SCAN-D4 gives the lowest MAD of 0.36 kcal/mol, showcasing on overall improved description of this kind of NCIs.

To evaluate if the good performance for non-covalent interactions transfers from the gas phase to solids, molecular crystals and their polymorphic forms provide useful test cases.^{77–79} Here, we investigate the lattice energy benchmark DMC8⁸⁰ shown in Table IV. The DMC8 benchmark contains a subset of the X23^{78,81–83} and ICE10⁸⁴ benchmark sets with accurate structures and corresponding highly accurate fixed node diffusion Monte Carlo (FN-DMC) results. Due to SCAN's tendency to overbind hydrogen bonded systems, such as ice polymorphs or hydrogen bonded molecular crystals, dispersion corrected SCAN was problematic for these systems. With the improved description of non-covalent interactions in r^2 SCAN-D4, this issue is mitigated and we find an overall improved MAD of 0.7 kcal/mol. This MAD is only half of the SCAN-D4 error of 1.5 kcal/mol for these systems and close to the very good performance of the hybrid PBE0-D4 of 0.5 kcal/mol.⁸⁵ Only

TABLE IV. Lattice energies (kcal/mol) of eight diverse molecular crystals compared to high-level.⁸⁰ Note the significant improvement from r^2 SCAN to r^2 SCAN-D4 for the dispersion-bound solids.

	Ref.	TPSS-D4	r^2 SCAN	r^2 SCAN-D4
Ice Ih	−14.2	−15.6	−14.6	−15.4
Ice II	−14.1	−14.6	−14.3	−15.4
Ice VIII	−13.7	−12.5	−13.4	−14.7
CO ₂	−6.7	−5.5	−4.7	−6.9
Ammonia	−8.9	−8.6	−8.1	−9.5
Benzene	−12.7	−12.0	−5.6	−12.3
Naphthalene	−18.8	−18.5	−7.5	−18.6
Anthracene	−25.2	−24.8	−9.9	−24.7
MD		0.3	4.6	−0.4
MAD		0.8	5.7	0.7
SD		0.9	6.0	0.8
AMAX		1.4	15.4	1.3

the ice polymorphs are systematically overbound by r^2 SCAN-D4, which is, however, a problem of many functionals^{86,87} and may be a self-interaction error.¹⁸ Both r^2 SCAN-D4 and SCAN-D4 yield similar results for the self-interaction subset (SIE4x4) of the GMTKN55, and therefore, a recent work investigating self-interaction corrections for SCAN might also be transferable to r^2 SCAN as well.⁸⁸ In contrast, the relative stability of the ice polymorph is reproduced correctly. The energy differences of ice II and ice VIII with respect to ice Ih are 0.03 kcal/mol and 0.70 kcal/mol, respectively, in good agreement with the reference values of 0.05 kcal/mol and 0.41 kcal/mol, respectively.

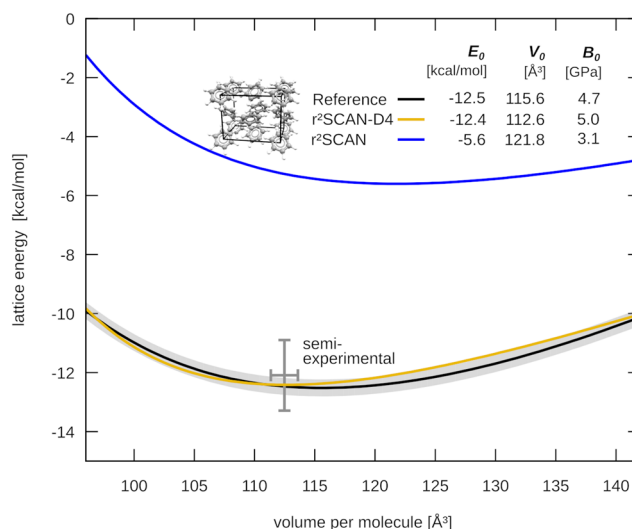


FIG. 5. Equation of state for the benzene crystal from r^2 SCAN-D4 compared to experimental measurements and high-level references taken from Ref. 80, and the gray area highlights the 1σ confidence interval.

The benzene crystal has been frequently used for electronic benchmark purposes.^{89–91} Here, we evaluated the equation of state (EOS) to compare with experimental measurements and the Muraghan EOS fit to the FN-DMC from Ref. 80. The resulting EOS is shown in Fig. 5 and agrees excellently with the high-level method as well as the experimental estimate. A slight underestimation of the unit cell volume by 2.6% and overestimation of the bulk modulus by 6.4% can be seen. To highlight once again the importance of London dispersion on properties beyond the mere energy, we report plain r^2 SCAN results as well. The r^2 SCAN EOS has a significant offset equilibrium volume that is overestimated by 5.4% and a bulk modulus underestimated by 34.0%.

IV. CONCLUSIONS

We have presented an accurate and robust combination of the non-empirical r^2 SCAN DFA with the state-of-the-art D4 dispersion correction. The resulting r^2 SCAN-D4 electronic structure method shows exceptional performance across several diverse categories of chemical problems assessed by thousands of high-level data points in a number of comprehensive benchmark sets. Included in the assessment were molecular thermochemistry for both main group and transition metal compounds, barrier heights, structure optimizations, lattice energies of molecular crystals, and both inter- and intramolecular non-covalent interactions of small to large systems, creating an extensive coverage of chemically relevant problems.

For the large GMTKN55 benchmark collection of about 1500 data points, r^2 SCAN-D4 is one of the most accurate meta-GGAs tested so far. Unlike the best meta-GGA on this set, the dispersion corrected B97M functional, r^2 SCAN-D4 can transfer this accuracy to chemically distinct systems such as metalorganic reactions. We find significant improvements in NCIs, which were one of the weak spots of SCAN based methods. More detailed analysis showed that improvements can mainly be found in the description of hydrogen and halogen bonded systems. The same trend is found for molecular crystals, where SCAN-D4's tendency to overbind is mostly resolved in r^2 SCAN-D4, giving close to hybrid DFT results for lattice energies.

We found r^2 SCAN-D4 to be an accurate and (more importantly) consistent DFA for a large variety of problems and chemical systems. The already good performance of the original SCAN functional is kept and systematically improved in r^2 SCAN, while the numeric stability is almost on par with the established GGA functionals. We were able to gain some insight into the improvement from SCAN over r SCAN to r^2 SCAN, where we can attribute the improved description of non-covalent interactions to the regularization in the step from SCAN to r SCAN and the improved thermochemistry and barrier heights to the constraint restoration in the step from r SCAN to r^2 SCAN. Like SCAN, r^2 SCAN is not fitted to molecules, so its accuracy in extensive molecular tests demonstrates the predictive power of its exact constraints and appropriate norms.

With r^2 SCAN-D4, a meta-GGA method is finally available that truly leverages the advantages of its rung in Jacob's ladder while retaining favorable numerical properties and fulfilling important exact constraints. We anticipate r^2 SCAN-D4 to be a valuable

electronic structure method with broad applications in computational chemistry and material science.

ACKNOWLEDGMENTS

We thank Stefan Grimme for valuable discussions. S.E. was supported by the DFG in the framework of the priority program 1807 "Control of London Dispersion Interactions in Molecular Chemistry." J.N., J.W.F., and J.S. acknowledge the support of the U.S. DOE, Office of Science, Basic Energy Sciences (Grant No. DE-SC0019350, core research). A.D.K. acknowledges the support of the U.S. DOE, Office of Science, Basic Energy Sciences, through Grant No. DE-SC0012575 to the Energy Frontier Research Center: Center for Complex Materials from First Principles. J.P.P. was supported by the U.S. National Science Foundation under Grant No. DMR-1939528 (CMMT with a contribution from CTMC).

DATA AVAILABILITY

The data that support the findings of this study are openly available at <https://github.com/awvwgk/r2scan-d4-paper> and from the corresponding author upon reasonable request.

REFERENCES

- 1 R. G. Parr and W. Yang, *Density-Functional Theory of Atoms and Molecules* (Oxford University Press, Oxford, 1989).
- 2 W. Kohn, "Electronic structure of matter—Wave functions and density functionals," *Rev. Mod. Phys.* **71**, 1253–1266 (1998).
- 3 K. Burke, "Perspective on density functional theory," *J. Chem. Phys.* **136**, 150901 (2012).
- 4 A. D. Becke, "Perspective: Fifty years of density-functional theory in chemical physics," *J. Chem. Phys.* **140**, 18A301 (2014).
- 5 R. J. Maurer, C. Freysoldt, A. M. Reilly, J. G. Brandenburg, O. T. Hofmann, T. Björkman, S. Lebègue, and A. Tkatchenko, "Advances in density-functional calculations for materials modeling," *Annu. Rev. Mater. Res.* **49**, 1–30 (2019).
- 6 J. P. Perdew and K. Schmidt, "Jacob's ladder of density functional approximations for the exchange-correlation energy," *AIP Conf. Proc.* **577**, 1–20 (2001).
- 7 J. Sun, A. Ruzsinszky, and J. P. Perdew, "Strongly constrained and appropriately normed semilocal density functional," *Phys. Rev. Lett.* **115**, 036402 (2015).
- 8 Y. Zhao and D. G. Truhlar, "A new local density functional for main-group thermochemistry, transition metal bonding, thermochemical kinetics, and non-covalent interactions," *J. Chem. Phys.* **125**, 194101 (2006).
- 9 R. Peverati and D. G. Truhlar, "M11-L: A local density functional that provides improved accuracy for electronic structure calculations in chemistry and physics," *J. Phys. Chem. Lett.* **3**, 117–124 (2012).
- 10 N. Mardirossian and M. Head-Gordon, "Characterizing and understanding the remarkably slow basis set convergence of several Minnesota density functionals for intermolecular interaction energies," *J. Chem. Theory Comput.* **9**, 4453–4461 (2013).
- 11 N. Mardirossian and M. Head-Gordon, "Mapping the genome of meta-generalized gradient approximation density functionals: The search for B97M-V," *J. Chem. Phys.* **142**, 074111 (2015).
- 12 L. Goerigk, "Treating London-dispersion effects with the latest Minnesota density functionals: Problems and possible solutions," *J. Phys. Chem. Lett.* **6**, 3891–3896 (2015).

- ¹³E. R. Johnson, A. D. Becke, C. D. Sherrill, and G. A. DiLabio, "Oscillations in meta-generalized-gradient approximation potential energy surfaces for dispersion-bound complexes," *J. Chem. Phys.* **131**, 034111 (2009).
- ¹⁴N. Mardirossian and M. Head-Gordon, "ωB97X-V: A 10-parameter, range-separated hybrid, generalized gradient approximation density functional with nonlocal correlation, designed by a survival-of-the-fittest strategy," *Phys. Chem. Chem. Phys.* **16**, 9904–9924 (2014).
- ¹⁵Y. Wang, X. Jin, H. S. Yu, D. G. Truhlar, and X. He, "Revised M06-L functional for improved accuracy on chemical reaction barrier heights, noncovalent interactions, and solid-state physics," *Proc. Natl. Acad. Sci. U. S. A.* **114**, 8487–8492 (2017).
- ¹⁶A. P. Bartók and J. R. Yates, "Regularized SCAN functional," *J. Chem. Phys.* **150**, 161101 (2019).
- ¹⁷J. W. Furness, A. D. Kaplan, J. Ning, J. P. Perdew, and J. Sun, "Accurate and numerically efficient r²SCAN meta-generalized gradient approximation," *J. Phys. Chem. Lett.* **11**, 8208–8215 (2020).
- ¹⁸K. Sharkas, K. Wagle, B. Santra, S. Akter, R. R. Zope, T. Baruah, K. A. Jackson, J. P. Perdew, and J. E. Peralta, "Self-interaction error overbinds water clusters but cancels in structural energy differences," *Proc. Natl. Acad. Sci. U. S. A.* **117**, 11283–11288 (2020).
- ¹⁹D. Mejía-Rodríguez and S. B. Trickey, "Spin-crossover from a well-behaved, low-cost meta-GGA density functional," *J. Phys. Chem. A* **124**, 9889–9894 (2020).
- ²⁰S. Grimme, A. Hansen, J. G. Brandenburg, and C. Bannwarth, "Dispersion-corrected mean-field electronic structure methods," *Chem. Rev.* **116**, 5105–5154 (2016).
- ²¹E. Caldeweyher, S. Ehlert, A. Hansen, H. Neugebauer, S. Spicher, C. Bannwarth, and S. Grimme, "A generally applicable atomic-charge dependent London dispersion correction," *J. Chem. Phys.* **150**, 154122 (2019).
- ²²D. Mejía-Rodríguez and S. B. Trickey, "Comment on 'Regularized SCAN functional' [J. Chem. Phys. 150, 161101 (2019)]," *J. Chem. Phys.* **151**, 207101 (2019).
- ²³A. P. Bartók and J. R. Yates, "Response to 'Comment on 'Regularized SCAN functional' [J. Chem. Phys. 151, 207101 (2019)]," *J. Chem. Phys.* **151**, 207102 (2019).
- ²⁴J. Sun, B. Xiao, Y. Fang, R. Haunschuld, P. Hao, A. Ruzsinszky, G. I. Csonka, G. E. Scuseria, and J. P. Perdew, "Density functionals that recognize covalent, metallic, and weak bonds," *Phys. Rev. Lett.* **111**, 106401 (2013).
- ²⁵J. G. Brandenburg, J. E. Bates, J. Sun, and J. P. Perdew, "Benchmark tests of a strongly constrained semilocal functional with a long-range dispersion correction," *Phys. Rev. B* **94**, 115144 (2016).
- ²⁶J. W. Furness and J. Sun, "Enhancing the efficiency of density functionals with an improved iso-orbital indicator," *Phys. Rev. B* **99**, 041119 (2019).
- ²⁷M. Levy and J. P. Perdew, "Hellmann-Feynman, virial, and scaling requisites for the exact universal density functionals. Shape of the correlation potential and diamagnetic susceptibility for atoms," *Phys. Rev. A* **32**, 2010–2021 (1985).
- ²⁸A. Görling and M. Levy, "Correlation-energy functional and its high-density limit obtained from a coupling-constant perturbation expansion," *Phys. Rev. B* **47**, 13105–13113 (1993).
- ²⁹L. Pollack and J. P. Perdew, "Evaluating density functional performance for the quasi-two-dimensional electron gas," *J. Phys.: Condens. Matter* **12**, 1239–1252 (2000).
- ³⁰P. S. Svendsen and U. von Barth, "Gradient expansion of the exchange energy from second-order density response theory," *Phys. Rev. B* **54**, 17402–17413 (1996).
- ³¹J. P. Perdew and Y. Wang, "Accurate and simple analytic representation of the electron-gas correlation-energy," *Phys. Rev. B* **45**, 13244–13249 (1992).
- ³²T. Aschebrock and S. Kümmel, "Ultranonlocality and accurate band gaps from a meta-generalized gradient approximation," *Phys. Rev. Res.* **1**, 033082 (2019).
- ³³F. Hofmann and S. Kümmel, "Molecular excitations from meta-generalized gradient approximations in the Kohn-Sham scheme," *J. Chem. Phys.* **153**, 114106 (2020).
- ³⁴D. Mejía-Rodríguez and S. B. Trickey, "Meta-GGA performance in solids at almost GGA cost," *Phys. Rev. B* **102**, 121109 (2020).
- ³⁵R. Sure and S. Grimme, *J. Chem. Theory Comput.* **11**, 3785–3801 (2015).
- ³⁶Wall time running on Intel® Xeon® CPU E3-1270 v5 @ 3.60 GHz using four cores.
- ³⁷The 6 radial points correspond to the default settings of Turbomole's grid m4.
- ³⁸An in-depth study of r2SCANs numerical behavior within PAW expansion is currently investigated.
- ³⁹J. Klimeš and A. Michaelides, "Perspective: Advances and challenges in treating van der Waals dispersion forces in density functional theory," *J. Chem. Phys.* **137**, 120901 (2012).
- ⁴⁰J. Hermann, R. A. DiStasio, and A. Tkatchenko, "First-principles models for van der Waals interactions in molecules and materials: Concepts, theory, and applications," *Chem. Rev.* **117**, 4714–4758 (2017).
- ⁴¹K. Berland, V. R. Cooper, K. Lee, E. Schröder, T. Thonhauser, P. Hyldgaard, and B. I. Lundqvist, "van der Waals forces in density functional theory: A review of the vdW-DF method," *Rep. Prog. Phys.* **78**, 066501 (2015).
- ⁴²O. A. Vydrov and T. Van Voorhis, "Nonlocal van der Waals density functional: The simpler the better," *J. Chem. Phys.* **133**, 244103 (2010).
- ⁴³R. Sabatini, T. Gorni, and S. de Gironcoli, "Nonlocal van der Waals density functional made simple and efficient," *Phys. Rev. B* **87**, 041108 (2013).
- ⁴⁴E. R. Johnson and A. D. Becke, "A post-Hartree-Fock model of intermolecular interactions," *J. Chem. Phys.* **123**, 024101 (2005).
- ⁴⁵E. R. Johnson and A. D. Becke, "A post-Hartree-Fock model of intermolecular interactions: Inclusion of higher-order corrections," *J. Chem. Phys.* **124**, 174104 (2006).
- ⁴⁶B. M. Axilrod and E. Teller, "Interaction of the van der Waals type between three atoms," *J. Chem. Phys.* **11**, 299–300 (1943).
- ⁴⁷Y. Muto, "Force between nonpolar molecules," *Proc. Phys. Soc. Jpn.* **17**, 629 (1943).
- ⁴⁸J. Rezáč, K. E. Riley, and P. Hobza, "S66: A well-balanced database of benchmark interaction energies relevant to biomolecular structures," *J. Chem. Theory Comput.* **7**, 2427 (2011).
- ⁴⁹M. S. Marshall, L. A. Burns, and C. D. Sherrill, "Basis set convergence of the coupled-cluster correction, $\delta_{\text{MP2}}^{\text{CCSD(T)}}$: Best practices for benchmarking noncovalent interactions and the attendant revision of the S22, NBC10, HBC6, and HSG databases," *J. Chem. Phys.* **135**, 194102 (2011).
- ⁵⁰D. E. Taylor, J. G. Ángyán, G. Galli, C. Zhang, F. Gygi, K. Hirao, J. W. Song, K. Rahul, O. Anatole von Lilienfeld, R. Podeszwa *et al.*, "Blind test of density-functional-based methods on intermolecular interaction energies," *J. Chem. Phys.* **145**, 124105 (2016).
- ⁵¹W. Hujo and S. Grimme, "Performance of non-local and atom-pairwise dispersion corrections to DFT for structural parameters of molecules with noncovalent interactions," *J. Chem. Theory Comput.* **9**, 308–315 (2013).
- ⁵²F. Furche, R. Ahlrichs, C. Hättig, W. Klopper, M. Sierka, and F. Weigend, "Turbomole," *Wiley Interdiscip. Rev.: Comput. Mol. Sci.* **4**, 91–100 (2014).
- ⁵³TURBOMOLE V7.5 2020, a development of University of Karlsruhe and Forschungszentrum Karlsruhe GmbH, 1989-2007, TURBOMOLE GmbH, since 2007; available from <http://www.turbomole.org>.
- ⁵⁴K. Eichkorn, O. Treutler, H. Öhm, M. Häser, and R. Ahlrichs, "Auxiliary basis sets to approximate Coulomb potentials," *Chem. Phys. Lett.* **240**, 283–289 (1995).
- ⁵⁵K. Eichkorn, F. Weigend, O. Treutler, and R. Ahlrichs, "Auxiliary basis sets for main row atoms and transition metals and their use to approximate Coulomb potentials," *Theor. Chem. Acc.* **97**, 119–124 (1997).
- ⁵⁶F. Weigend, F. Furche, and R. Ahlrichs, "Gaussian basis sets of quadruple zeta quality for atoms H to Kr," *J. Chem. Phys.* **119**, 12753–12762 (2003).
- ⁵⁷G. Kresse and J. Hafner, "Ab initio molecular dynamics for liquid metals," *Phys. Rev. B* **47**, 558 (1993).
- ⁵⁸G. Kresse and J. Furthmüller, "Efficiency of ab-initio total energy calculations for metals and semiconductors using a plane-wave basis set," *Comput. Mater. Sci.* **6**, 15 (1996).
- ⁵⁹P. E. Blöchl, "Projector augmented-wave method," *Phys. Rev. B* **50**, 17953 (1994).
- ⁶⁰G. Kresse and D. Joubert, "From ultrasoft pseudopotentials to the projector augmented-wave method," *Phys. Rev. B* **59**, 1758 (1999).
- ⁶¹S. Grimme, J. G. Brandenburg, C. Bannwarth, and A. Hansen, "Consistent structures and interactions by density functional theory with small atomic orbital basis sets," *J. Chem. Phys.* **143**, 054107 (2015).

- ⁶²M. Bühl and H. Kabrede, “Geometries of transition-metal complexes from density-functional theory,” *J. Chem. Theory Comput.* **2**, 1282–1290 (2006).
- ⁶³M. Piccardo, E. Penocchio, C. Puzzarini, M. Biczysko, and V. Barone, “Semi-experimental equilibrium structure determinations by employing B3LYP/SNSD anharmonic force fields: Validation and application to semirigid organic molecules,” *J. Phys. Chem. A* **119**, 2058–2082 (2015).
- ⁶⁴É. Brémond, M. Savarese, N. Q. Su, Á. J. Pérez-Jiménez, X. Xu, J. C. Sancho-García, and C. Adamo, “Benchmarking density functionals on structural parameters of small-/medium-sized organic molecules,” *J. Chem. Theory Comput.* **12**, 459–465 (2016).
- ⁶⁵Optimized r^2 SCAN-D4/def2-QZVP geometries of the LMGB35, HMGB11, and TMC32 sets, statistical performance of the LMGB35, HMGB11, TMC32, CCse21, ^{63,64} GMTKN55, S30L, L7, C40x10 sets are provided at <https://github.com/awwngk/r2scan-d4-paper>.
- ⁶⁶C. Adamo and V. Barone, “Toward reliable density functional methods without adjustable parameters: The PBE0 model,” *J. Chem. Phys.* **110**, 6158–6170 (1999).
- ⁶⁷J. Tao, J. P. Perdew, V. N. Staroverov, and G. E. Scuseria, “Climbing the density functional ladder: Nonempirical meta generalized gradient approximation designed for molecules and solids,” *Phys. Rev. Lett.* **91**, 146401 (2003).
- ⁶⁸J. P. Perdew, K. Burke, and M. Ernzerhof, “Generalized gradient approximation made simple,” *Phys. Rev. Lett.* **77**, 3865–3868 (1996); Erratum, **78**, 1396 (1997).
- ⁶⁹L. Goerigk, A. Hansen, C. A. Bauer, S. Ehrlich, A. Najibi, and S. Grimme, “A look at the density functional theory zoo with the advanced GMTKN55 database for general main group thermochemistry, kinetics and noncovalent interactions,” *Phys. Chem. Chem. Phys.* **19**, 32184 (2017).
- ⁷⁰A. Najibi and L. Goerigk, “DFT-D4 counterparts of leading meta-generalized-gradient approximation and hybrid density functionals for energetics and geometries,” *J. Comput. Chem.* **41**, 2562 (2020).
- ⁷¹For a subset of the GMTKN55 not all of the published benchmark results with the SCAN functional were reproducible. Therefore, we reevaluated SCAN on the complete GMKTN55.
- ⁷²S. Dohm, A. Hansen, M. Steinmetz, S. Grimme, and M. P. Checinski, “Comprehensive thermochemical benchmark set of realistic closed-shell metal organic reactions,” *J. Chem. Theory Comput.* **14**, 2596–2608 (2018).
- ⁷³P. Pernot and A. Savin, “Using the Gini coefficient to characterize the shape of computational chemistry error distributions,” [arXiv:2012.09589](https://arxiv.org/abs/2012.09589) (2020).
- ⁷⁴R. Sedlak, T. Janowski, M. Pitoňák, J. Řezáč, P. Pulay, and P. Hobza, “Accuracy of quantum chemical methods for large noncovalent complexes,” *J. Chem. Theory Comput.* **9**, 3364–3374 (2013).
- ⁷⁵M. K. Kesharwani, D. Manna, N. Sylvetsky, and J. M. L. Martin, “The X40 \times 10 halogen bonding benchmark revisited: Surprising importance of $(n - 1)d$ subvalence correlation,” *J. Phys. Chem. A* **122**, 2184–2197 (2018).
- ⁷⁶Y. S. Al-Hamdani, P. R. Nagy, D. Barton, M. Kállay, J. G. Brandenburg, and A. Tkatchenko, “Interactions between large molecules: Puzzle for reference quantum-mechanical methods,” [arXiv:2009.08927](https://arxiv.org/abs/2009.08927)[physics.chem-ph] (2020).
- ⁷⁷A. Otero-de-la-Roza, B. H. Cao, I. K. Price, J. E. Hein, and E. R. Johnson, “Predicting the relative solubilities of racemic and enantiopure crystals by density-functional theory,” *Angew. Chem., Int. Ed.* **53**, 7879–7882 (2014).
- ⁷⁸A. M. Reilly and A. Tkatchenko, “Understanding the role of vibrations, exact exchange, and many-body van der Waals interactions in the cohesive properties of molecular crystals,” *J. Chem. Phys.* **139**, 024705 (2013).
- ⁷⁹G. J. O. Beran, “Modeling polymorphic molecular crystals with electronic structure theory,” *Chem. Rev.* **116**, 5567–5613 (2016).
- ⁸⁰A. Zen, J. G. Brandenburg, J. Klimeš, A. Tkatchenko, D. Alfè, and A. Michaelides, “Fast and accurate quantum Monte Carlo for molecular crystals,” *Proc. Natl. Acad. Sci. U. S. A.* **115**, 1724–1729 (2018).
- ⁸¹A. Otero-de-la-Roza and E. R. Johnson, “A benchmark for non-covalent interactions in solids,” *J. Chem. Phys.* **137**, 054103 (2012).
- ⁸²A. Ambrosetti, A. M. Reilly, R. A. DiStasio, and A. Tkatchenko, “Long-range correlation energy calculated from coupled atomic response functions,” *J. Chem. Phys.* **140**, 18A508 (2014).
- ⁸³D. J. Carter and A. L. Rohl, “Benchmarking calculated lattice parameters and energies of molecular crystals using van der Waals density functionals,” *J. Chem. Theory Comput.* **10**, 3423–3437 (2014).
- ⁸⁴J. G. Brandenburg, T. Maas, and S. Grimme, “Benchmarking DFT and semiempirical methods on structures and lattice energies for ten ice polymorphs,” *J. Chem. Phys.* **142**, 124104 (2015).
- ⁸⁵E. Caldeweyher, J.-M. Mewes, S. Ehlert, and S. Grimme, “Extension and evaluation of the D4 London-dispersion model for periodic systems,” *Phys. Chem. Chem. Phys.* **22**, 8499–8512 (2020).
- ⁸⁶B. Santra, J. Klimeš, A. Tkatchenko, D. Alfè, B. Slater, A. Michaelides, R. Car, and M. Scheffler, “On the accuracy of van der Waals inclusive density-functional theory exchange-correlation functionals for ice at ambient and high pressures,” *J. Chem. Phys.* **139**, 154702 (2013).
- ⁸⁷J. G. Brandenburg, A. Zen, D. Alfè, and A. Michaelides, “Interaction between water and carbon nanostructures: How good are current density functional approximations?,” *J. Chem. Phys.* **151**, 164702 (2019).
- ⁸⁸K. Wagle, B. Santra, P. Bhattarai, C. Shahi, M. R. Pederson, K. A. Jackson, and J. P. Perdew, “Self-interaction correction in water-ion clusters,” *J. Chem. Phys.* (to be published); [arXiv:2012.13469](https://arxiv.org/abs/2012.13469).
- ⁸⁹S. Wen and G. J. O. Beran, “Accurate molecular crystal lattice energies from a fragment QM/MM approach with on-the-fly ab initio force field parametrization,” *J. Chem. Theory Comput.* **7**, 3733–3742 (2011).
- ⁹⁰M. R. Kennedy, A. R. McDonald, A. E. DePrince, M. S. Marshall, R. Podeszwa, and C. D. Sherrill, “Communication: Resolving the three-body contribution to the lattice energy of crystalline benzene: Benchmark results from coupled-cluster theory,” *J. Chem. Phys.* **140**, 121104 (2014).
- ⁹¹W. J. Hehre, R. Ditchfield, and J. A. Pople, *J. Chem. Phys.* **56**, 2257 (1972).